doi:10.1038/nature11784

Methods

The ECHO-G model and simulations

The ECHO-G model[29] consists of the 19-level ECHAM4 atmospheric model and 20-level HOPE-G ocean circulation model. The horizontal resolutions are approximately 3.75° (atmosphere) and 2.8° (ocean) in both latitude and longitude with a refined latitudinal spacing of 0.5° in the tropical ocean. To enable the coupled model to sustain a climate close to real present day climate with minimal drift, constant (in time) fields of heat and fresh-water fluxes with zero net spatial averages were added at the atmosphere-ocean interface.

Two millennial integrations[28] with the ECHO-G model were analyzed: a 1000-year control (free) simulation generated using fixed annually cycling forcing set at present-day values and a forced run, named ERIK, covering the period 1000-1990, which is externally forced by solar variability, the effective radiative effects from stratospheric volcanic aerosols, and greenhouse gas concentrations in the atmosphere including CO_2 and CH_4 for the period AD 1000-1990. The volcanic forcing was parameterized in this simulation as a simple reduction of the annual mean solar constant, starting in the year with a volcanic eruption and usually lasting a couple of years.

The forced integration starts from an imbalanced initial condition at 900 AD[28], which may affect the reliability of the precipitation in the first 200 years[20]. An

additional analysis using the data for the period of AD 1200-1850 shows that the leading EOF mode does not change appreciably, so it is not significantly affected by initial conditions (Fig. S8). The total solar irradiance (TSI) used in the forced run is based on ^{14}C and ^{10}Be production rates compiled by Bard et al[31]. The TSI is scaled to be about a 3.5 W m^{-2} (0.25%) change from the Maunder minimum (AD 1647-1715) to the modern period (AD 1950-2000). Recent evaluations suggest a much weaker TSI forcing with an increase of ~1.3 W m^{-2} (0.1%) from the Maunder minimum to today[32]. In any case both this forcing and that due to volcanism are highly uncertain. Although the amplitude of solar forcing fluctuations used (Fig. 1a) is higher than more recent estimates, the simulated northern hemisphere mean temperature is within the range of uncertainties deduced from various reconstructions[15]**.** Checks on the sensitivity of the solution to this forcing, especially the forced mode, would be desirable. Its amplitude would surely change, but we do not anticipate qualitative changes in the coupled precipitation-SST pattern.

Two additional forced simulations with the ECHO-G model were also analyzed. One is the greenhouse-gas (GHG) forced run for the period 1860-2000 with initial condition selected from a long preindustrial control simulation. Nineteen GHGs were used including CO_2, CH_4, N_2O[18]. The other is the Emissions Scenarios (SRES) balance across all sources (A1B) run from 1990 to 2100 with 720 ppm stabilization at 2100.

Removal of Internal Mode of Variability

To identify the internal decadal variation mode, we performed a Principal

Component (PC) analysis of the 11-year running mean precipitation. The leading PC fluctuates irregularly and intermittently on decadal time scales (Fig. S3a). The corresponding spatial pattern (Empirical Orthogonal Function, EOF) displays large variances in the tropical Pacific and is nearly identical to the leading EOF mode obtained from the control run without any external forcing (Fig. S3b), suggesting that this variability is rooted in internal processes within the climate system. The associated SST and 850 hPa winds indicate a decadal warming in the equatorial central-western Pacific and cooling in the eastern Pacific (Fig. S4).

To detect major patterns of forced decadal variation, we first removed the internal mode component of the precipitation from the ERIK run, and then applied a Maximum Covariance Analysis (MCA[22]) to the precipitation and SST fields for the period AD 1000-1850.

Statistical test for the difference of the regressions

Two slopes of the regressions are denoted by b_1 and b_2. To test whether the difference between the two slopes is not due to sampling errors, we use the $t-$test

$$t(n_1+n_2-4)=\frac{b_1-b_2}{S_{yx}\sqrt{\frac{1}{S_{x1}}+\frac{1}{S_{x2}}}}\quad , \qquad (1)$$

where S_{x1} and S_{x2} are the sum of squares for x for the first and second groups, respectively and

$$S_{yx}=\sqrt{\frac{S_{y1}+S_{y2}-b_1^2S_{x1}-b_2^2S_{x2}}{n_1+n_2-4}}\,, \qquad (2)$$

where S_{y1} and S_{y2} are the sum of squares for y for the first and second groups, n_1 and n_2 are sample size for these two groups.

In the case of the two regressions shown in Fig. 2 for the ERIK run, $t(95) = 25.8$, indicating that the difference between the two slopes is statistically significant at the 95% confidence level.

References

1. Bard, E., Raisbeck, G., Yiou, F. & Jouzel, J. Solar irradiance during the last 1200 years based on cosmogenic nuclides. *Tellus*, **52B**, 985–992 (2000).
2. Foukal P., Fröhlich, C., Spruit, H. & Wigley, T. M. L. Variations in solar luminosity and their effect on the Earth's climate. *Nature*, **443**, 161–166 (2006).

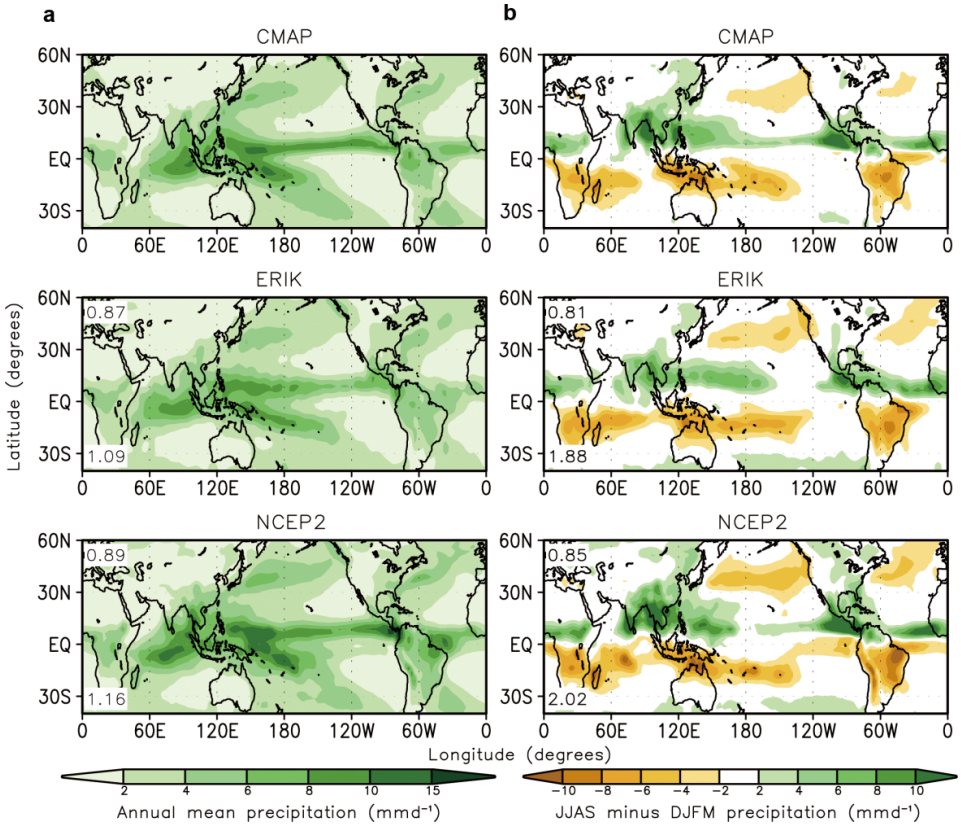

Figure S1 | Validation of the model precipitation climatology by comparison of the observed and simulated climatology of global precipitation rate (mm d^{-1}). a, annual mean and **b,** the leading mode of the annual cycle measured by JJAS (June through September) minus DJFM (December through following March) derived from CMAP (top), ECHO-G ERIK forced run (middle), and NCEP-2 reanalysis (bottom). CMAP and NCEP-2 reanalysis climatological data were derived for the period 1979–2004. The 25-year climatology simulated in the ECHO-G ERIK forced run was derived for the period AD 1965–1990. The numbers shown in the upper-left corners and the lower-left corners indicate the pattern correlation coefficients with the CMAP observational analysis and root mean square errors (adopted from Liu et al. 2009).

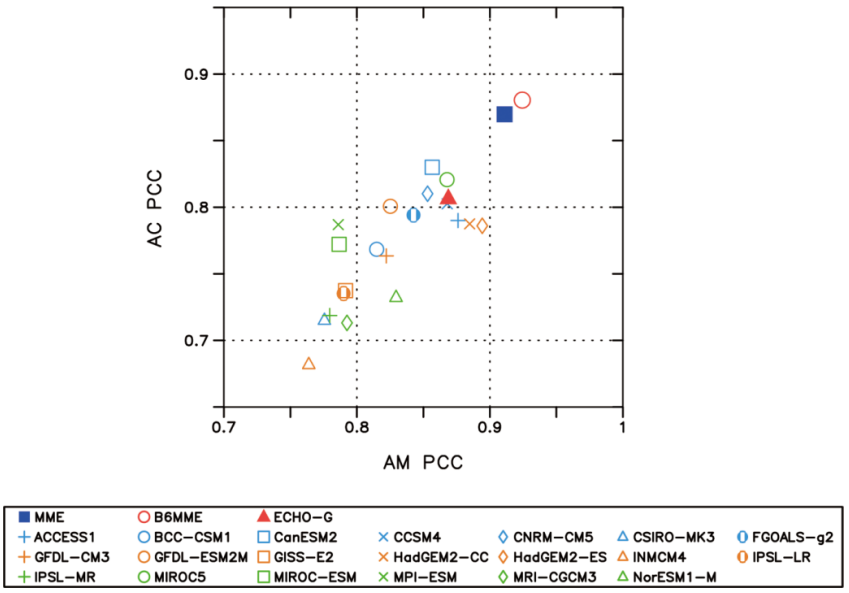

Figure S2 | The precipitation climatology of the ECHO-G model in comparison with 20 CMIP5 CGCMs. The abscissa is the pattern correlation coefficient (PCC) for the annual mean and the ordinate is the PCC of the combined first and second annual cycle of precipitation. The CMIP 5 model climatology is for the 26 years 1980-2005 and for ECHO-G it is the 30-year mean from 1961-1990. The spatial domain is 0^{o}-360^{o}E, 60^{o}S-60^{o}N. The observed precipitation data were obtained from combining CMAP and GPCP data. The ECHO-G model performance is comparable to the best CMIP5 models. All models are outperformed by multi-model ensemble means: MME denotes the mean of all 20 CMIP5 models and B6MME denotes the mean of the 6 best models.

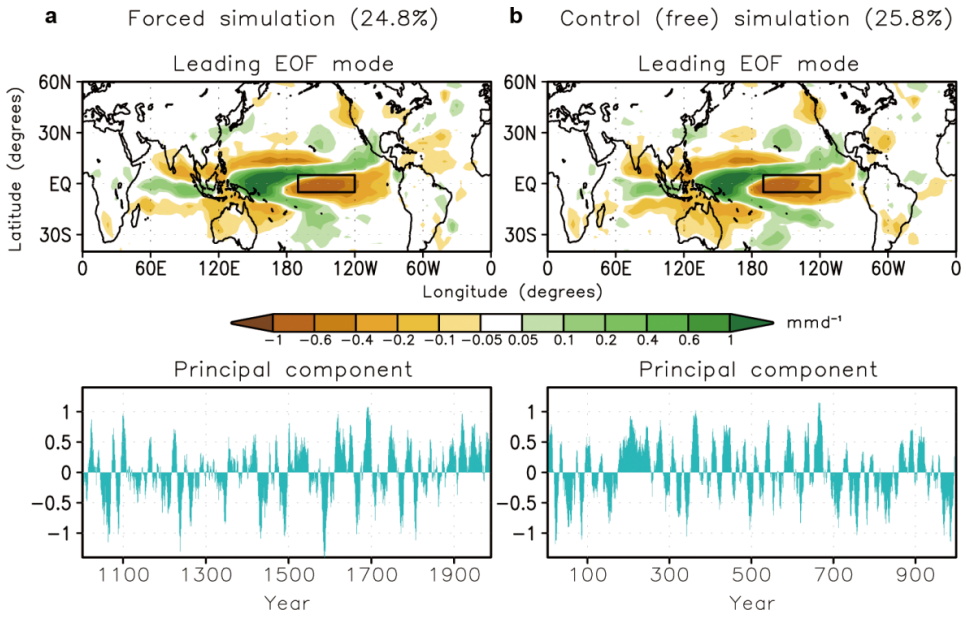

Figure S3 | The internal mode of global precipitation obtained from the ECHO-G simulation. a, forced simulation from 1000-1990 and **b,** control (free) simulation. The upper panels show the spatial structures (leading EOF) and the lower panels the principal component (PC) time series. The data used are 11-year running mean time series and a cosine area weighting was applied. The numbers on the top of panel **a** and **b** denote the fractional variances of the leading EOF modes. The boxes in the upper panels indicate the NINO3.4 region.

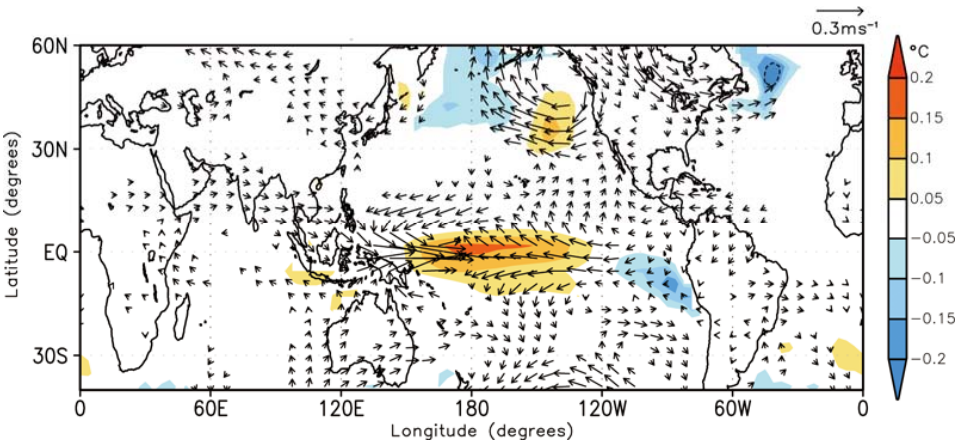

Figure S4 | SST and 850hPa winds regressed on the PC1 of the precipitation in the forced simulation. Shown are wind vectors that are significant above 95% confidence level in either the zonal or meridional component.

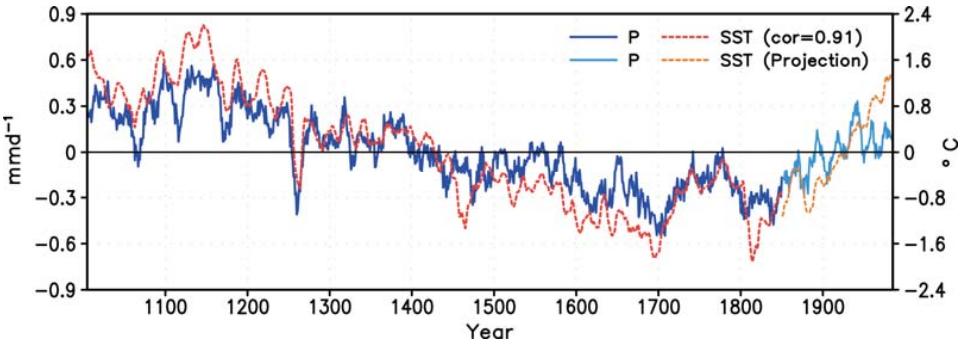

Figure S5 | The time expansion coefficients for the solar-volcanic forced MCA mode shown in Fig. 3b during 1000-1850. Projected coefficients of precipitation and SST are also shown from 1851 to 1990.

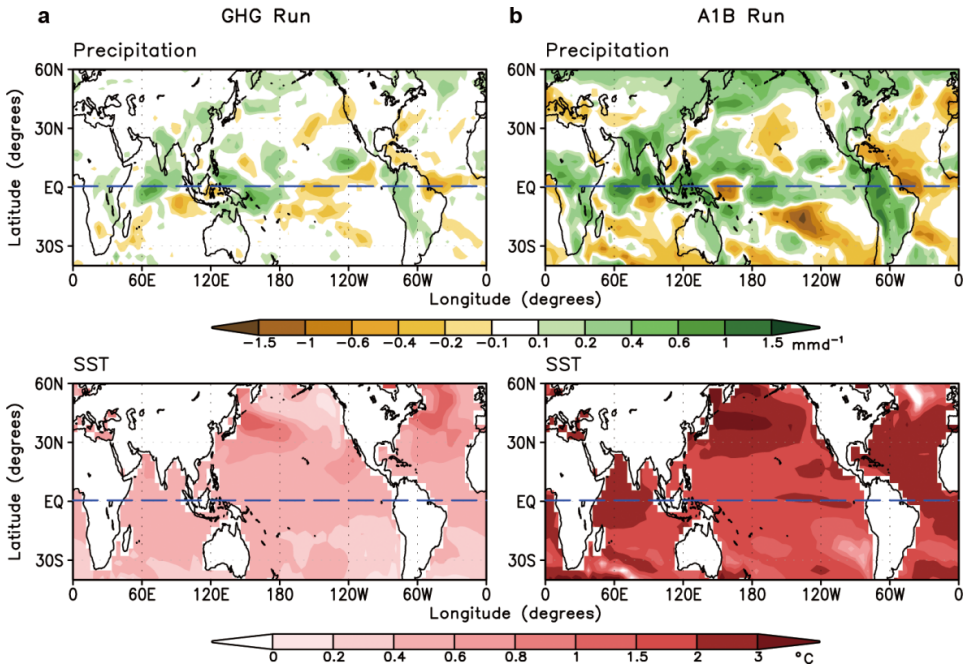

Figure S6 | Comparison of the precipitation (upper) and SST (lower) changes in two GHG only forcing runs with the ECHO-G model. a, The GHG run with observed GHG forcing for the period 1970-1989 relative to the period 1860-1879. **b,** The Emissions Scenarios (SRES) balance across all sources (A1B) run for the period 2070-2099 relative to the period 1990-2019. The blue long-dashed line indicates the equator.

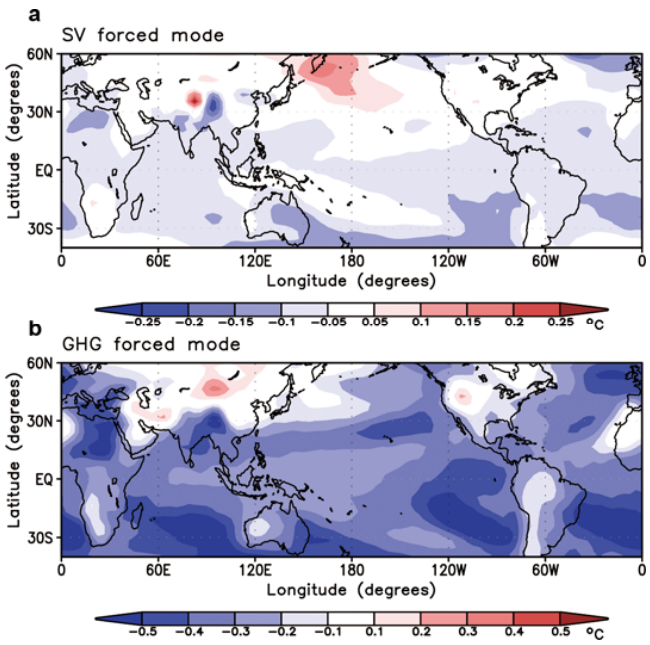

Figure S7 | Atmospheric static stability associated with the SV and GHG modes. Shown are (T850-T500) regressed onto **a,** the SV forced mode derived from the ERIK forced run for 1000-1850 and **b,** the GHG mode derived from the GHG forced run with observed GHG forcing for 1860-2000, both with the same ECHO-G model. Negative values stand for reduced (T850-T500) or increased static stability.

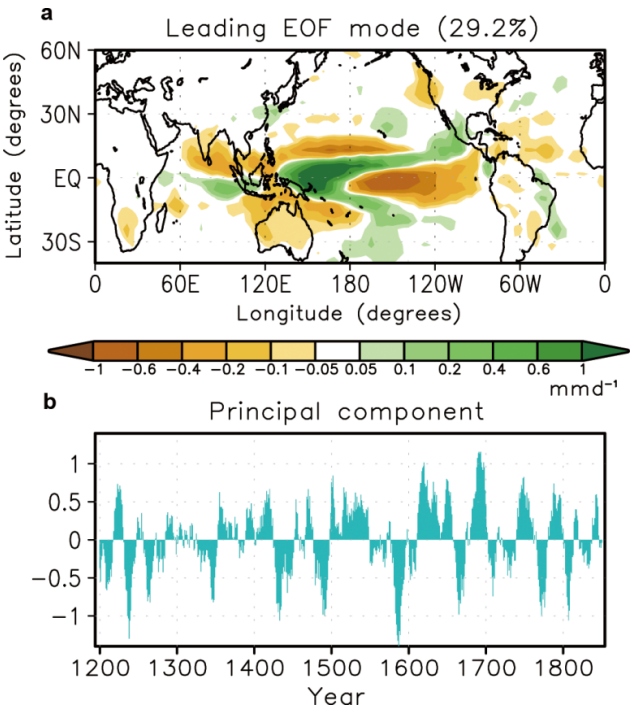

Figure S8 | Leading EOF mode for the period 1200-1850. The spatial structure (EOF1, upper) and principal component (PC1, lower) of global precipitation derived by using the ECHO-G model forced simulation data from 1200-1850. The data used are cosine area weighted 11-year running mean time series. Leaving out the first 200 years data does not significantly change the leading EOF mode.